

# A Change in Inflammatory Footprint Precedes Plaque Instability: A Systematic Evaluation of Cellular Aspects of the Adaptive Immune Response in Human Atherosclerosis

R. A. van Dijk, MD; A. J. F. Duiniveld, MD; A. F. Schaapherder, MD, PhD; A. Mulder-Stapel, BSc; J. F. Hamming, MD, PhD; J. Kuiper, MD, PhD; O. J. de Boer, MD, PhD; A. C. van der Wal, MD, PhD; F. D. Kolodgie, PhD; R. Virmani, MD; J. H. N. Lindeman, MD, PhD

**Background**—Experimental studies characterize adaptive immune response as a critical factor in the progression and complications of atherosclerosis. Yet, it is unclear whether these observations translate to the human situation. This study systematically evaluates cellular components of the adaptive immune response in a biobank of human aortas covering the full spectrum of atherosclerotic disease.

**Methods and Results**—A systematic analysis was performed on 114 well-characterized perirenal aortic specimens with immunostaining for T-cell subsets (CD3/4/8/45RA/45RO/FoxP3) and the Th1/non-Th1/Th17 ratio (CD4<sup>+</sup>T-bet<sup>+</sup>/CD4<sup>+</sup>T-bet<sup>-</sup>/CD4<sup>+</sup>/interleukin-17<sup>+</sup> double staining). CD20 and CD138 were used to identify B cells and plasma cells, while B-cell maturation was evaluated by AID/CD21 staining and expression of lymphoid homeostatic CXCL13. Scattered CD4 and CD8 cells with a T memory subtype were found in normal aorta and early, nonprogressive lesions. The total number of T cells increases in progressive atherosclerotic lesions ( $\approx$ 1:5 CD4/CD8 T-cell ratio). A further increase in medial and adventitial T cells is found upon progression to vulnerable lesions. This critical stage is further hallmarked by de novo formation of adventitial lymphoidlike structures containing B cells and plasma cells, a process accompanied by transient expression of CXCL13. A dramatic reduction of T-cell subsets, disappearance of lymphoid structures, and loss of CXCL13 expression characterize postruptured lesions. FoxP3 and Th17 T cells were minimally present throughout the atherosclerotic process.

**Conclusions**—Transient CXCL13 expression, restricted presence of B cells in human atherosclerosis, along with formation of nonfunctional extranodal lymphoid structures in the phase preceding plaque rupture, indicates a “critical” change in the inflammatory footprint before and during plaque destabilization. (*J Am Heart Assoc.* 2015;4:e001403 doi: 10.1161/JAHA.114.001403)

**Key Words:** adaptive immunity • aorta • atherosclerosis • vulnerable plaque • inflammation • necrotic core • neovessel

Atherosclerosis is a highly dynamic<sup>1,2</sup> metabolic disease with a strong inflammatory component.<sup>3–5</sup> Compelling evidence, largely based on data derived from murine models

of atherosclerotic disease, implies extensive involvement of the adaptive immune response in the initiation, progression, and complications of atherosclerotic disease.<sup>6</sup> As a consequence, the adaptive immune response is considered a potential target for medical interventions.

An open question is how these observations translate to the human situation. There are fundamental immunological and inflammatory differences between mice and humans.<sup>7–9</sup> Moreover, murine models of accelerated atherosclerotic disease require an immunologic background with exaggerated Th1-cell responsiveness in order for atherosclerosis to develop.<sup>8,9</sup> Hence, observations from mouse models may be skewed toward Th1 response. Extrapolation of the murine data is further complicated by absence of vulnerable lesion formation in the current models of atherosclerotic disease. As a result, data on a possible involvement of the adaptive immune response in the advanced stages of atherosclerotic disease are missing.

From the Departments of Vascular Surgery (R.A.V.D., A.J.F.D., A.M.-S., J.F.H., J.H.N.L.) and Transplantation Surgery (A.F.S.), Leiden University Medical Center, Leiden, The Netherlands; Gorlaeus Laboratories, Division of Biopharmaceutics, Leiden Academic Centre for Drug Research, Leiden, The Netherlands (J.K.); Department of Pathology, Academic Medical Center, Amsterdam, The Netherlands (O.J.D.B., A.C.V.D.W.); CVPath Institute Inc., Gaithersburg, MD (F.D.K., R.V.).

**Correspondence to:** J. H. N. Lindeman, MD, PhD, Department of Vascular Surgery, Leiden University Medical Center, P. O. Box 9600, 2300 RC Leiden, The Netherlands. E-mail: lindeman@lumc.nl

Received November 28, 2014; accepted January 24, 2015.

© 2015 The Authors. Published on behalf of the American Heart Association, Inc., by Wiley Blackwell. This is an open access article under the terms of the Creative Commons Attribution-NonCommercial License, which permits use, distribution and reproduction in any medium, provided the original work is properly cited and is not used for commercial purposes.

**Table 1.** Demographic Data of the 114 Studied Aortic Samples

	Male	Female
N	64	50
Mean age, y (SD)	49.4 (14.3)	43.8 (17.3)
Mean length, cm (SD)	179.9 (11.9)	166.6 (12.1)
Mean weight, kg (SD)	80.1 (16.3)	64.9 (15.3)
Mean BMI, kg/m <sup>2</sup> (SD)	24.8 (3.1)	22.9 (4.4)
Number of patients with known history of nicotine abuse	21 (36.8%)	17 (39.5%)
Number of patients with known history of hypertension*	13 (22.8%)	10 (23.3%)
Number of patients with known diabetes	0 (0.0%)	1 (2.3%)
Cause of death		
Severe head trauma	11 (17.1%)	7 (14.0%)
Cerebral vascular accident	8 (12.5%)	10 (20.0%)
Subarachnoid bleeding	15 (23.4%)	14 (28.0%)
Cardiac arrest	7 (10.9%)	0 (0.0%)
Trauma	1 (1.5%)	1 (2.0%)
Other	6 (9.3%)	3 (6.0%)
Unknown	16 (25.0%)	15 (30%)
Medication		
Antihypertensives	11 (19.3%)	6 (14.0%)
Statins	1 (1.7%)	1 (2.3%)
Anticoagulants	1 (1.7%)	2 (4.7%)
Other	5 (8.8%)	8 (18.6%)
None	31 (54.4%)	22 (51.2%)
Unknown	11 (19.3%)	9 (20.9%)

\*Known antihypertensive medication or systolic blood pressure >140 mm Hg and diastolic >90 mm Hg in the period preceding death. BMI indicates body mass index.

**Table 2.** Antibodies Used in the Present Study

Antibody, Clone	Host Isotype; Subclass	Specificity	Pretreatment		Dilution	Reference/Source
CD3, polyclonal	Rabbit	Pan T cells	10x Tris/EDTA	pH 9.2	1:200	DAKO
CD4, 4B12	Mouse, IgG1-κ	T-helper cells	10x Tris/EDTA	pH 9.2	1:200	DAKO
CD8, C8/144B	Mouse, IgG1-κ	Cytotoxic T cells	10x Tris/EDTA	pH 9.2	1:200	DAKO
CD45RA, HI100	Mouse, IgG2b-κ	Naive T cells	Citrate	pH 6.0	1:2000	BioLegend
CD45RO, UCHL1	Mouse, IgG2a-κ	Memory T cells	Citrate	pH 6.0	1:1000	BioLegend
CD20, L26	Mouse	Pan B cells	Citrate	pH 6.0	1:1000	DAKO
CD21, IF8(4)	Mouse, IgG1-κ	Follicular dendritic Cells, mature B cells	Citrate	pH 6.0	1:400	DAKO
CD138, MI15	Mouse	Plasma cells	10x Tris/EDTA	pH 9.2	1:1000	DAKO
CCR7, ab191575	Rabbit, polyclonal	Activated T-lymphocytes	Citrate	pH 9.2	1:200	Abcam
Tbet, polyclonal	Rabbit, sc-21003	T-helper1 cells	10x Tris/EDTA	pH 9.2	1:800	Santa Cruz
IL-17, polyclonal	Goat	Th-17 cells	–	pH 9.0	1:50	R&D
FoxP3, clone 236A/E7	Mouse	Regulatory T cells	–	pH 9.0	1:50	Abcam
CXCL13, cat no AF801	Goat	Lymphorganogenic chemokine	Citrate	pH 6.0	1:100	R&D
Anti-AID, EK2 5G9	Rat	Activation-induced cytidine deaminase	Citrate	pH 6.0	1:16.000	Cell Signalling

AID indicates activation-induced cytidine deaminase; Ig, immunoglobulin; IL, interleukin.

Available human data, on the other hand, largely rely on surgical specimens. Yet, it is important to note that this material generally represents the final stages of the disease process.<sup>10,11</sup> As such, data from these human studies are not representative for the earlier and intermediate phases of atherosclerotic disease; hence, knowledge of the nature of the adaptive immune response in the human atherosclerotic process is limited.

Given the above considerations, we regarded an evaluation of the adaptive immune response within the process of atherosclerotic lesion formation, progression, and stabilization to be relevant. To that end, we performed comprehensive and systematic histological assessment of cellular aspects of the adaptive immune response in tissue samples from a biobank of arterial tissue that covers the full spectrum of human atherosclerotic disease. Results from this explorative study confirm an extensive and dynamic presence of cellular components of the adaptive immunity in the human atherosclerotic process, and reveal profound changes in the inflammatory footprint immediately prior to and during the process of plaque destabilization.

## Materials and Methods

### Patients and Tissue Sampling

Tissue sections were selected from a tissue bank of aortic wall patches that were obtained during liver, kidney, and

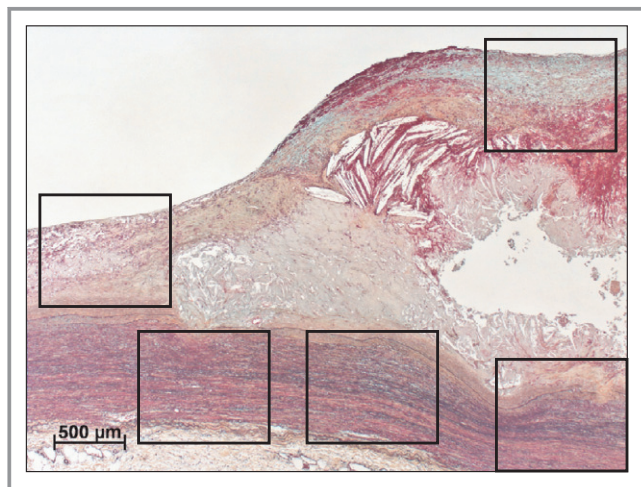


**Figure 1.** Example of the regions of interest as used for the assessment of immunolocalization of T cells (and T-cell subset), B cells, and plasma cells in a healed rupture. The regions of interest are drawn in the fibrous cap, in 1 of the shoulders and 3 times in the media in this particular example. For every lesion (normal or ruptured), a total of 9 images were made (3 in the intima, 3 in the media, and 3 in the adventitia) and the immunostaining was quantitatively assessed with an image-processing program (Image J; plug-in Cellcounter).

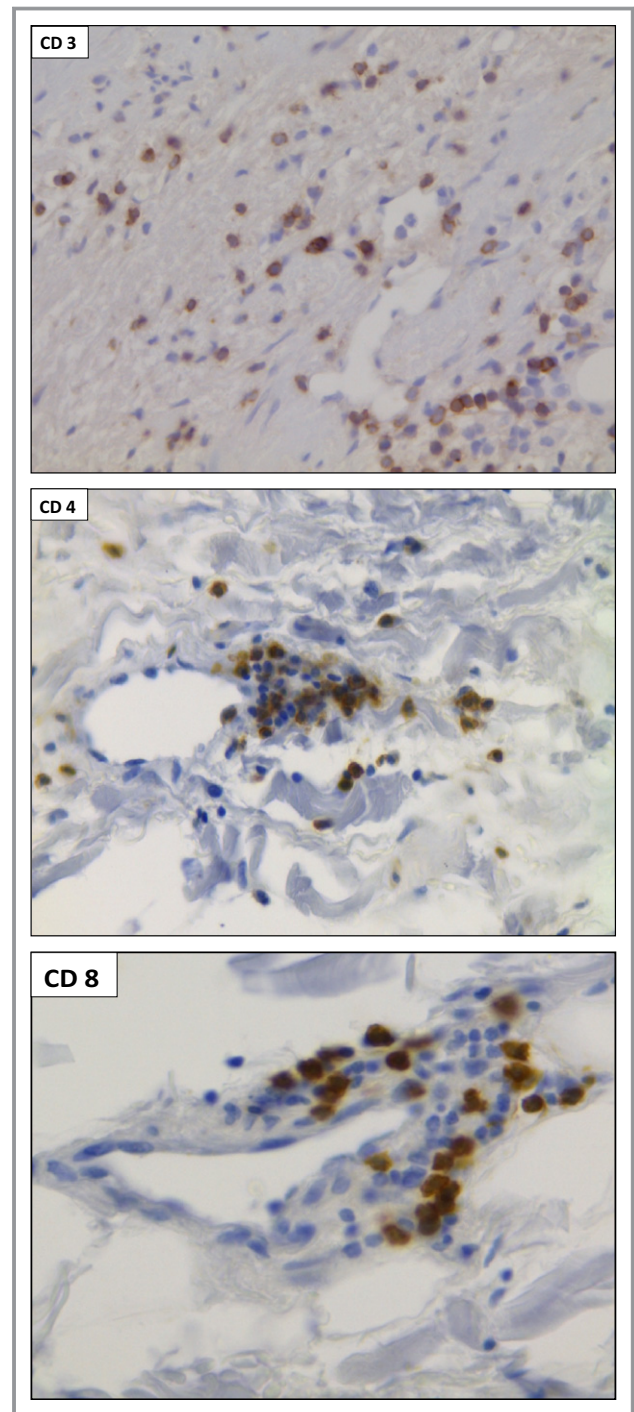


**Figure 2.** High-resolution examples of the immunohistochemical staining for CD3, CD4, and CD8 cells. The high-resolution images are examples of the quality of the immunohistochemical staining for CD3, CD4, and CD8. All images were taken at a  $\times 400$  magnification at the medial adventitial border. Within all the images, one can see the clear positively stained T cells mainly located near the vasa vasorum. All sections were developed with Diaminobenzidine (DAB) and counterstained with Mayer's hematoxylin.

pancreas transplantation with grafts derived from cadaveric donors. Details of this bank have been described previously by van Dijk et al<sup>12</sup>. All patches were from grafts that were eligible for transplantation (ie, all donors met the criteria set by The Eurotransplant Foundation). Due to national regulations, only transplantation-relevant data for donation are available, as such background information on the specimens is limited. Sample collection and handling was performed in accordance with the guidelines of the Medical and Ethical Committee in Leiden, Netherlands and the code of conduct of the Dutch Federation of Biomedical Scientific Societies (<http://www.federa.org/?s=1&m=82&p=0&v=4#827>).

Each tissue block in the bank was Movat and H&E stained and classified according to the modified American Heart Association (AHA) classification as proposed by Virmani et al by 2 independent observers with no knowledge of the characteristics of the aortic patch.<sup>12,13</sup> The tissue block showing the most advanced plaque was used for further studies. In order to obtain balanced and representative study groups, we selected the first 100 aortic wall samples from the tissue bank. Due to the fact that the vulnerable lesions (ie, thin cap fibroatheroma and plaque ruptures) were under-represented, we randomly selected several aortic wall samples classified as vulnerable lesions from the remaining 250 patches in order to obtain approximately 10 to 12 samples from each atherosclerotic stage. A total of 114 cases were

selected for further examination. Demographic data and the causes of death are summarized in Table 1.

### Characterization of the Lesions and Histological Definitions

Aortic samples not showing any signs of intimal thickening and intimal inflammation were classified as normal. The other samples were classified based on the most advanced lesion type present in the section. Lesions were defined as adaptive intimal thickening, intimal xanthoma, pathological intimal thickening, early fibroatheroma, late fibroatheroma, thin-cap fibroatheroma, acute plaque rupture, healed plaque rupture, and fibrotic calcified plaque. Detailed descriptions concerning a complete overview on plaque processing, morphological analysis, and additional information concerning the studied population are provided in van Dijk et al<sup>12</sup>.

### Immunohistochemistry

All specimens used for immunohistochemistry (IHC) were washed in PBS, formalin fixed, and decalcified (Kristensens solution), and paraffin embedded using standard procedures. The details of the antibodies used for IHC are listed in Table 2. Conjugated biotinylated horse anti-mouse (1:400 dilution; Vector laboratories, Amsterdam, the Netherlands) or Envi-

**Table 3.** Histological Classification of Aortic Tissue According to the Modified American Heart Association Classification Proposed by Virmani et al

Morphological Description	Abbreviation	Male		Female		Total
		N	Mean Age (SD)	N	Mean Age (SD)	N
Normal aorta	N	7	23.8 (18.9)	5	10.0 (3.7)	12
Nonprogressive intimal lesions						
Adaptive intimal thickening	AIT	5	40.5 (10.0)	5	30.4 (9.0)	10
Intimal xanthoma	IX	7	37.3 (10.0)	5	34.2 (14.8)	12
Progressive atherosclerotic lesions						
Pathological intimal thickening	PIT	5	46.0 (8.9)	7	55.4 (11.5)	12
Early fibroatheroma	EFA	7	50.9 (5.9)	5	46.0 (3.5)	12
Late fibroatheroma	LFA	5	55.0 (3.6)	7	51.1 (11.6)	12
Vulnerable atherosclerotic lesions						
Thin-cap fibroatheroma	TCFA	7	57.2 (5.2)	4	60.3 (5.7)	11
Plaque rupture	PR	7	56.9 (2.6)	3	45.0 (13.1)	10
Stabilizing lesions						
Healing rupture	HR	8	58.1 (11.1)	4	57.0 (0)	12
Fibrotic calcified plaque	FCP	6	62.7 (6.8)	5	53.0 (11.4)	11
		64	49.4 (14.3)	50	43.8 (17.3)	114

AIT indicates adaptive intimal thickening; EFA, early fibroatheroma; FCP, fibrotic calcified plaque; HR, healed rupture; IX, Intimal xanthoma; LFA, late fibroatheroma; N, normal; PIT, pathological intimal thickening; PR, plaque rupture; SD, standard deviation; TCFA, thin cap fibroatheroma.

sion+ System–horseradish peroxidase–labeled polymer anti-mouse/anti-rabbit (prediluted; Dako, Heverlee, Belgium) functioned as secondary antibodies. Sections were developed with Nova Red or DAB and counterstained with Mayer's hematoxylin or methyl green. Positive and negative controls were always included and performed by adding or omitting the primary antibody on 3-aminopropyltriethoxysilane slides containing human tonsils.

The Foxp3/CD3 and interleukin-17/CD3 double staining was performed to identify regulatory T cells and Th17 cells, respectively (Table 1). Conjugated polymer anti-mouse/anti-rabbit (Immunologic) functioned as secondary antibodies. After the goat-derived anti-interleukin-17 incubation, a rabbit anti-goat secondary antibody (Southern Biotech, Birmingham, AL) served as a bridge reagent for the next step with alkaline phosphatase anti-rabbit polymer (Immunologic, Duiven, the Netherlands). All immunohistochemical stainings were performed as previously described.<sup>14</sup> Despite many attempts and various techniques, we did not succeed in using GATA-3 as the T-helper 2 marker. We therefore had to turn to double staining for CD4/Tbet to identify the T-helper lineage (Lineage: Th1=CD4<sup>+</sup>/Tbet<sup>+</sup> and non-Th1=CD4<sup>+</sup>/Tbet<sup>-</sup>) having regard to the provision that non-Th1 may also include Th0, Th17, and Th22 populations.

### Assessment of Immunolocalization of T Cells (and T-Cell Subset), B Cells, and Plasma Cells

The tissue block showing the most advanced plaque was used for further studies. When the aortic sample contained more than 1 lesion, the most advanced lesion on the slide was used. The lesion was defined as the area between the endothelium and the first elastic lamina over a distance of 1 mm. In the presence of a necrotic core, the distance was expanded with another 500  $\mu$ m on both sides of the necrotic core to include the adjacent shoulder region.<sup>12</sup> The regions of interest were the intima (and in the presence of an early or late necrotic core, the intima was divided into a cap and both shoulder regions), the media, and the adventitia (Figure 1). Within the regions of interest (ie, intima, media, and adventitia), 3 representative adjacent images were made at a  $\times 200$  magnification. A total of 9 images per atherosclerotic lesion were separately analyzed from the lesion. Immunostaining intensity was quantitatively assessed with an image-processing program (Image J; plug-in Cellcounter). Representative examples of the immunological stainings are provided in Figure 2.

### Statistical Analysis

Data in figures are presented as mean $\pm$ SEM. Spearman's correlation was used to demonstrate the relationship

between the amount of positive cells in the intima, media, and adventitia within 1 phase of the atherosclerotic disease and compared with the previous and/or next

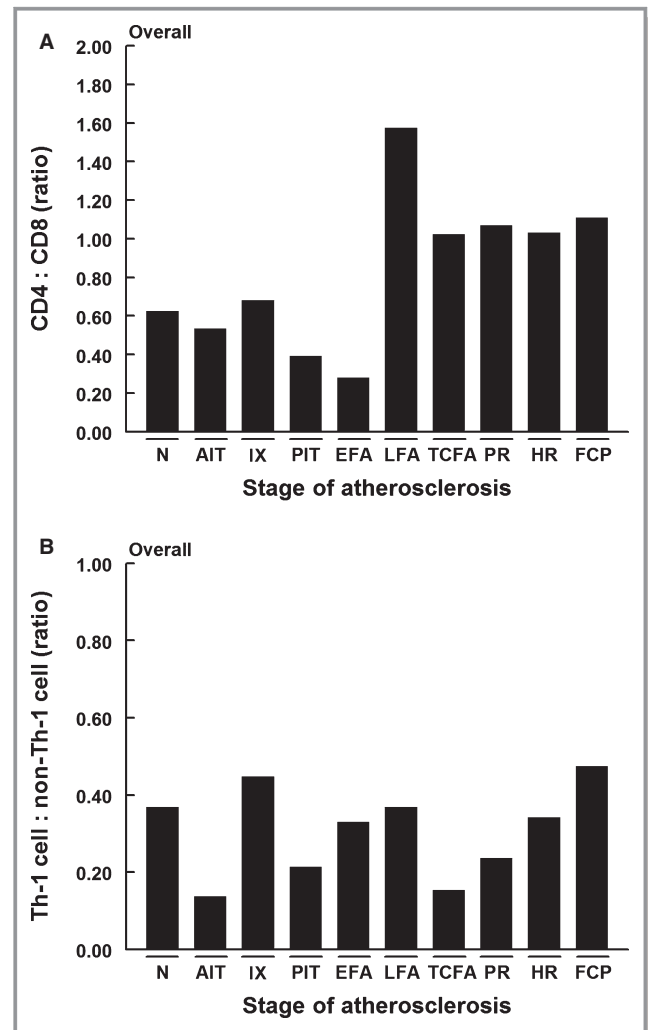


**Figure 3.** The CD4/CD8 and Th1/non-Th1 ratio per stage of atherosclerosis. A, The number of CD8 cells dominate the overall T-cell count in normal aortas and in the early stages of atherosclerosis up until the early fibroatheroma. In late fibroatheroma, vulnerable atherosclerosis (ie, thin-cap fibroatheroma and plaque ruptures), and postruptured plaques, the total number of CD4 and CD8 cells are practically in balance. B, Non-Th1 cells dominate the T-helper lineage not only in normal aortas, but also during the entire development of atherosclerotic lesions. Within thin-cap fibroatheroma, the non-Th1 cells dominate the Th1 cells with a factor 5 and as the lesion stabilizes, the Th1/non-Th1 cell ratio returns to 0.4–0.5 as seen in normal aortas. The solid bars represent the mean number of CD4 (A) or Th1 (B) cells per stage of atherosclerosis divided by the mean number of CD8 (A) or non-Th1 (B) cells per stage of atherosclerosis. AIT indicates adaptive intimal thickening; EFA, early fibroatheroma; FCP, fibrotic calcified plaque; HR, healed plaque rupture; IX, intimal xanthoma; LFA, late fibroatheroma; N, normal; PIT, pathological intimal thickening; PR, acute plaque rupture; TCFA, thin-cap fibroatheroma.

phase in atherosclerosis (SPSS 20.0; Chicago, IL). The study population consisted of 114 individuals. However, during the staining process some tissue samples were lost.

Therefore, the total number of samples for each staining may be less than 114. The Wilcoxon–Mann–Whitney test was used to analyze the non-normally distributed data of

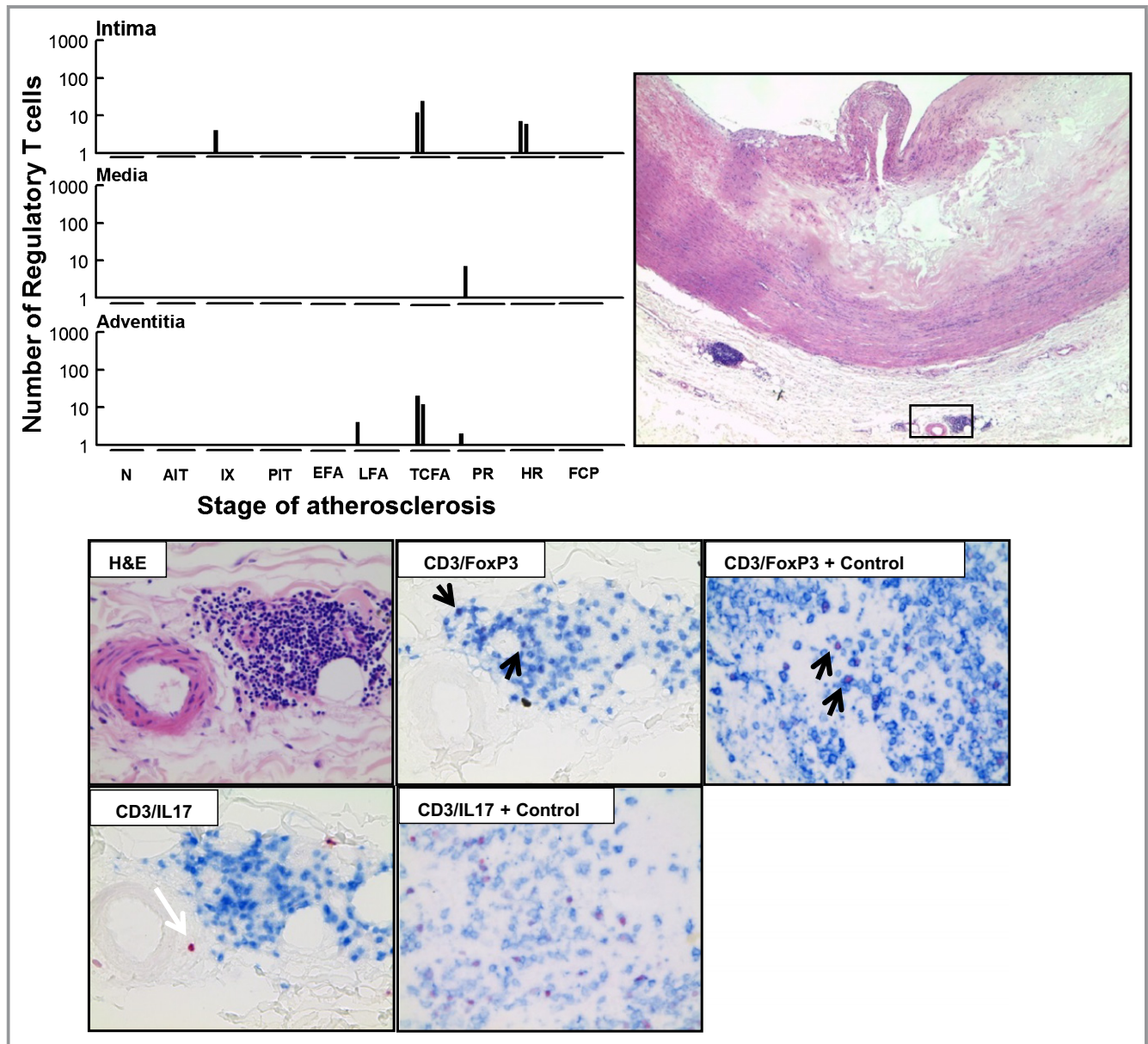


**Figure 4.** Number of regulatory T cells within the various layers of the aortic wall per stage of atherosclerosis. Only 1 aortic sample with an intimal xanthoma stained positive for FoxP3<sup>+</sup> T cells (4 scattered cells). Within the aortic samples classified as a thin-cap fibroatheroma, 2 lesions showed 12 and 24 FoxP3<sup>+</sup> T cells in the intima with 20 and 12 FoxP3<sup>+</sup> T cells, respectively, in the adjacent adventitia. A few scattered FoxP3<sup>+</sup> T cells were seen in the intima of 2 healed ruptured plaques. The additional figures show a hematoxylin and eosin (H&E)–stained adventitial follicle in a thin-cap fibroatheroma with the consecutive sections stained for regulatory T cells (CD3<sup>+</sup>/FoxP3<sup>+</sup>) and Th17 cells (CD3<sup>+</sup>/interleukin [IL]17<sup>+</sup>). There are a limited number of regulatory T cells (black arrows) in the vulnerable phase and Th17 cells were not identified. A few scattered CD3<sup>-</sup>/IL17<sup>+</sup> cells (white arrow) were seen in the adventitia that, as previous studies showed, can be addressed to macrophages.<sup>15</sup> A human tonsil (not associated with the aortic biobank) functioned as a positive control for the CD3/IL17 staining and showed numerous Th17 cells. Ferangi blue was used to develop CD3 and alkaline phosphatase for FoxP3 and IL17. The solid bars represent the number of FoxP3<sup>+</sup> T cells within the various layers of the aorta per stage of atherosclerosis. Total number of cases: 97 (N [9], AIT [9], IX [11], PIT [11], EFA [10], LFA [9], TCFA [9], PR [10], HR [8] and FCP [11]). For a detailed description concerning the classification, see the Materials and Methods section. All images were taken at a ×400 magnification. AIT indicates adaptive intimal thickening; EFA, early fibroatheroma; FCP, fibrotic calcified plaque; HR, healed plaque rupture; IX, intimal xanthoma; LFA, late fibroatheroma; N, normal; PIT, pathological intimal thickening; PR, acute plaque rupture; TCFA, thin-cap fibroatheroma.

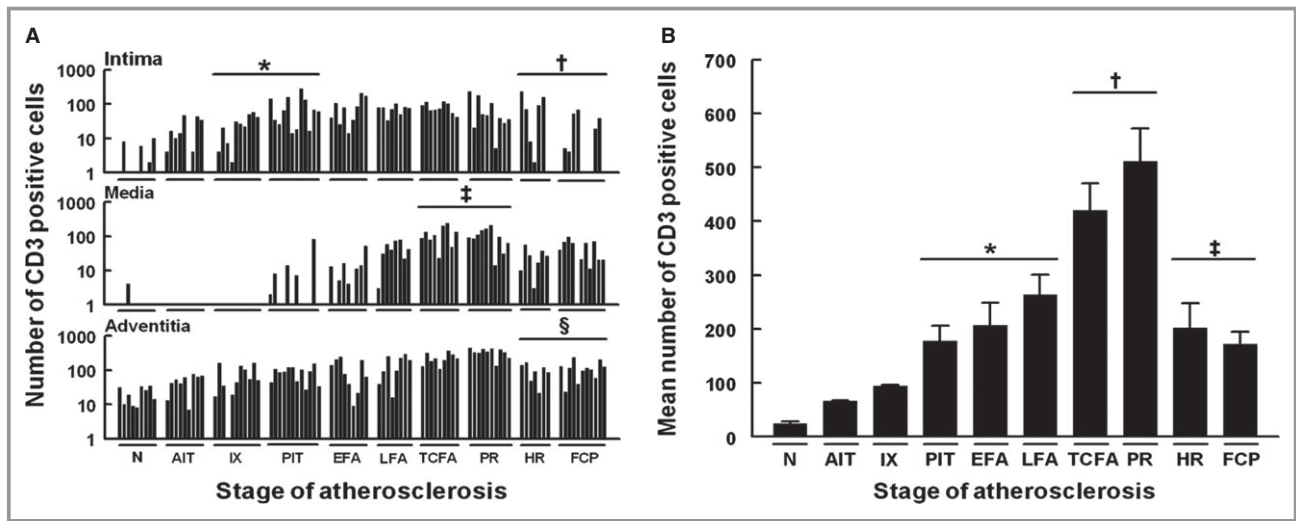


**Figure 5.** Number of CD3<sup>+</sup>, CD4<sup>+</sup>, and CD8<sup>+</sup> T cells within the various layers of the aortic wall. A, Intimal CD3<sup>+</sup> T cells are present in all stages of atherosclerosis. There is a significant influx of CD3<sup>+</sup> T cells in intimal xanthomas and pathological intimal thickening when compared to normal aortic wall samples ( $*P<0.009$ ). The number stabilizes as the lesion becomes vulnerable (viz, TCFA and PR). A significant decrease ( $†P<0.014$ ) is seen in the stabilizing lesions (viz, HR and FCP) compared to vulnerable lesions (viz, TCFA and PR). The media remains clear of CD3<sup>+</sup> T cells until pathological intimal thickening and shows a remarkable increase in CD3<sup>+</sup> expressing T cells ( $‡P<0.0001$ ) in vulnerable lesions. There are an increasing number of CD3<sup>+</sup> T cells in the adventitia with advancing atherosclerosis. Stabilized plaques are hallmarked by a significant decrease in adventitial CD3<sup>+</sup> T cells ( $§P<0.0001$ ) when compared to the vulnerable lesions. B, The total number of CD3<sup>+</sup> T cells in all vascular layers increases with advancing atherosclerosis. Progressive atherosclerotic lesions (viz, PIT, EFA, and LFA) show significantly more CD3<sup>+</sup> T cells compared to nonprogressive lesions (AIT and IX;  $*P<0.0001$ ). A further increase is seen in vulnerable lesions ( $†P<0.0001$ ), whereas lesion stabilization is hallmarked by a dramatic decrease ( $‡P<0.0001$ ). Total number of cases in (A) and (B): 95 (N [9], AIT [9], IX [11], PIT [12], EFA [9], LFA [8], TCFA [9], PR [10], HR [7], and FCP [11]). C, The intima remains practically devoid of CD4<sup>+</sup> T cells up until late fibroatheroma. There is a significant increase of T-helper cells in vulnerable lesions compared to PIT, EFA, and LFA followed by a significant decrease in stabilizing lesions ( $*P<0.008$ ;  $†P<0.004$ ). Similar patterns are seen within the media and adventitia ( $‡P<0.0001$ ;  $§P<0.003$ ;  $¶P<0.002$ ; and  $\#P<0.008$ ). D, T-helper cells significantly increase in progressive and vulnerable lesions in comparison to PIT, EFA, and LFA followed by a decrease in stabilized lesions ( $*P<0.021$ ;  $†P<0.0001$ ; and  $‡P<0.001$ ). Total number of cases in (C) and (D): 91 (N [8], AIT [9], IX [11], PIT [11], EFA [8], LFA [10], TCFA [9], PR [9], HR [7] and FCP [9]). E, Cytotoxic T cells are more abundantly present in the intima in the progressive stages of atherosclerosis ( $*P<0.001$ ) when compared to normal, AIT and IX. The media and adventitia show an increasing number of cytotoxic T cells within progressive atherosclerotic lesions (PIT, EFA, and LFA) compared to the prior phases followed by a significant rise within the vulnerable plaques and a significant decrease as the lesions stabilize ( $†P<0.0001$ ;  $‡P<0.0001$ ;  $§P<0.0001$ ; and  $¶P<0.0001$ ). F, The total number of cytotoxic T cells follows a similar pattern to that of the T-helper lineage in (B): a significant increase within progressive and vulnerable lesions followed by a decrease in stabilized lesions ( $*P<0.002$ ;  $†P<0.0001$ , and  $‡P<0.0001$ ). Total number of cases in (E) and (F): 96 (N [9], AIT [9], IX [10], PIT [12], EFA [10], LFA [10], TCFA [9], PR [10], HR [8] and FCP [9]). The vertical axis of (A), (C), and (E) is presented as a log-scale. Each solid bar in (A), (C), and (E) represents the number of positively stained T cells within the intima, media, and adventitia of 1 aortic plaque. The solid bars in (B), (D), and (F) represent the mean total number of cells within the entire aortic wall per stage of atherosclerosis  $\pm$ SEM. AIT indicates adaptive intimal thickening; EFA, early fibroatheroma; HR, healed rupture; FCP, fibrotic calcified plaque; IX, intimal xanthoma; LFA, late fibroatheroma; N, normal; PIT, pathological intimal thickening; PR, plaque rupture; TCFA, thin-cap fibroatheroma. For a detailed description concerning the classification, see the Materials and Methods section.

the mean total number of cells within each atherosclerotic phase, and the Kruskal–Wallis test was used to control for a type 1 error. A value of  $P<0.05$  was considered statistically significant.

## Results

### Studied Population

Characteristics of the studied population are provided in Table 1. The male/female ratio was evenly distributed

(57% male), as was the mean age for each sex ( $\approx 49$  years). There was a strong correlation between donor age and atherosclerosis progression<sup>12</sup> (Table 3). The mean donor age for the aortic wall samples classified as normal was 23 years, whereas the mean age for aortas with fibrotic calcified plaques, representing the final stage of the disease, was 62 years. Nearly 40% of patients had a known history of smoking, and 2 patients received statin therapy. Twenty-three patients had a known history of hypertension; 17 of these patients received antihypertensive medication.

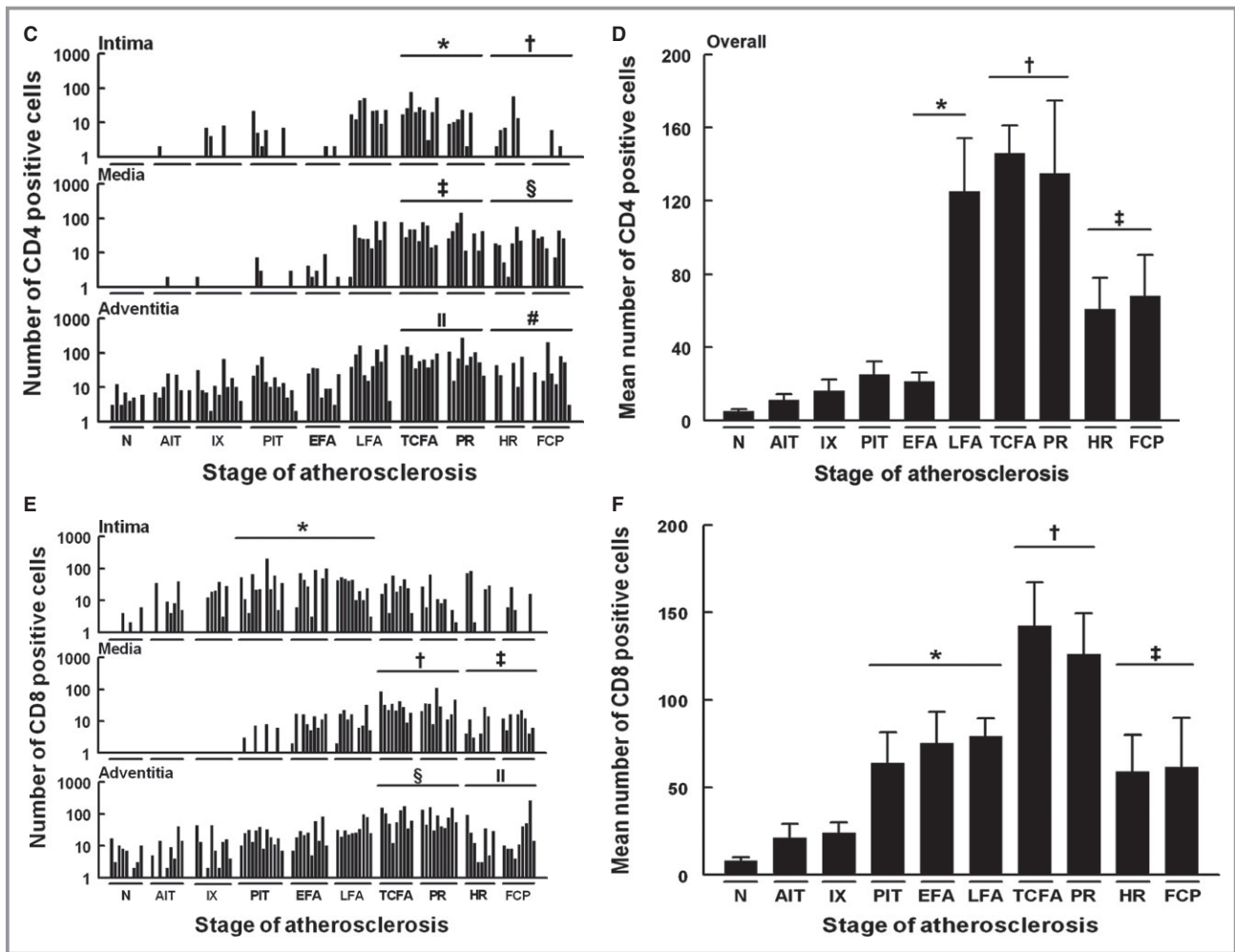


Figure 5. Continued.

### Normal Aorta and Nonprogressive Atherosclerotic Lesions

The intima and media layers of the normal (nonatherosclerotic) aortic wall are devoid of CD3<sup>+</sup> T cells (Figures 3 through 10). Scattered T cells found at the medial–adventitial border are mainly CD45RO<sup>+</sup> (memory) T cells. The CD4<sup>+</sup> (Thelper) to CD8<sup>+</sup> (cytotoxic) T-cell ratio is approximately 1:2 (Figure 3A). Th<sub>1</sub> cells and non-Th1 cells were also expressed in a 1:2 ratio (Figure 3B).

Naïve T cells (CD45RA<sup>+</sup>), regulatory T cells (CD3<sup>+</sup>/FoxP3<sup>+</sup>), Th17 cells (CD3<sup>+</sup>/IL17A<sup>+</sup>), B cells (CD20<sup>+</sup>), and plasma cells (CD138<sup>+</sup>) are all absent in aortas classified as normal.

Isolated T cells in the thickened intima, and progressive numbers of T cells in the medial/adventitial border characterize so-called nonprogressive lesions (ie, adaptive intimal thickening and intimal xanthomas). Memory T cells remain the dominant phenotype, and the subset ratios remains unchanged (CD4<sup>+</sup>/8<sup>+</sup>; Th1/Th2). Regulatory T cells, Th17

cells, naïve T cells, B cells, and plasma cells are absent in these early lesions (Figure 4).

### Progressive Atherosclerotic Lesions

A significant increase is seen in intimal CD3<sup>+</sup> T cells ( $P<0.0001$ ) in progressive lesions (early fibroatheroma and late fibroatheroma) with beginning infiltration of the medial wall as well. The predominance of cytotoxic T cells persists (CD4<sup>+</sup>: CD8<sup>+</sup> T-cell ratio 1:5) in the early fibroatheroma, and T-helper cells are dominated by the Th<sub>1</sub> lineage at a 1:3 ratio. Transition from an early to late fibroatheroma stage is accompanied by the accumulation of T cells in the intima shoulder regions of the lesion, and the CD4<sup>+</sup>/CD8<sup>+</sup> T-cell ratio shifts from 1:5 in early fibroatheroma to ≈1.5:1 in late fibroatheroma (Figures 3 through 9).

Memory T cells remain the dominant phenotype in advanced lesions, yet scattered naïve T cells (CD45RA<sup>+</sup>) start

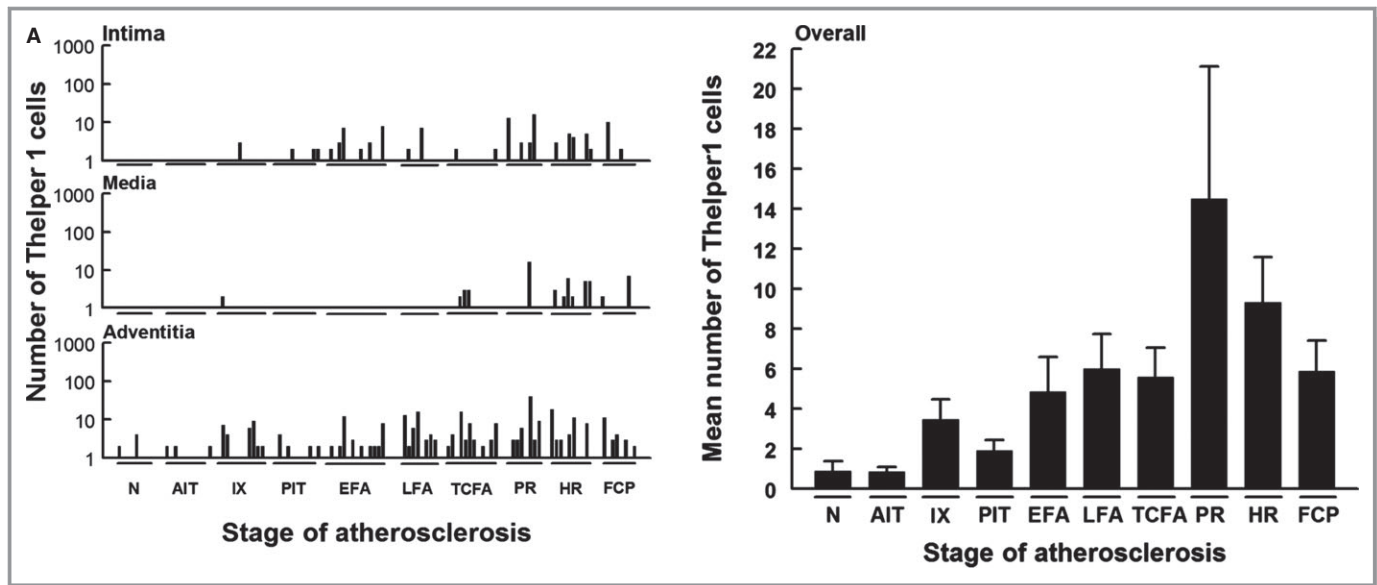


**Figure 6.** Number of Thelper1 and non-Thelper1 cells within the various layers of the aortic wall. A, There is a gradual increase in Thelper1 cells in the intima and adventitia with advancing atherosclerotic lesions. An increase is seen in the amount of Thelper1 cells within ruptured plaques; note the fact that these cells are mainly located in the adventitia. Total number of cases in (A): 97 (N [9], AIT [9], IX [11], PIT [11], EFA [12], LFA [8], TCFA [12], PR [8], HR [9] and FCP [8]). B, There are far more non-Thelper1 cells within the aortic wall compared to the number of Thelper1 cells. However, the same gradual increase in number is seen as the atherosclerotic lesions progress toward the vulnerable thin-cap fibroatheroma. Again, an increase is seen within ruptured plaques. Total number of cases in (B): 98 (N [8], AIT [10], IX [11], PIT [10], EFA [12], LFA [9], TCFA [12], PR [8], HR [10] and FCP [8]). C, Illustrative images of the adventitia adjacent to the intimal plaque in the various stages of the atherosclerotic process with CD4/Tbet double-staining corresponding with the presented graphs (A and B). Thelper1 cells are identified by staining positive for CD4 (brown; diaminobenzidine chromogen) and Tbet (methylgreen). Non-Thelper1 cells are CD4 positive and Tbet negative. Note that there are numerous cells that only stain Tbet positive. The vertical axis of the figures with the intima, media, and adventitia separated is presented as a log-scale and the solid bars represent the number of Thelper1 or non-Thelper1 cells within the various layers of 1 aortic plaque. The solid bars in the adjacent figures represent the mean total number of Th1 cells or non-Th1 cells within the entire aortic wall  $\pm$ SEM. AIT indicates adaptive intimal thickening; EFA, early fibroatheroma; HR, healed rupture; FCP, fibrotic calcified plaque; IX, intimal xanthoma; LFA, late fibroatheroma; N, normal; PIT, pathological intimal thickening; PR, plaque rupture; TCFA, thin-cap fibroatheroma. For a detailed description concerning the classification, see the Materials and Methods section. All images were taken at  $\times 400$  magnification.

to appear within the medial–adventitial border in lesions classified as early fibroatheroma. A further increase in naïve T cells and T memory cells is seen in late fibroatheroma with a notable accumulation of T cells alongside infiltrating vasa vasorum in the outer layers of the media underlying the necrotic core. In general, B cells and plasma cells are absent, although present in a minority of individuals (Figure 9). Regulatory T cells and Th17 cells are not identified in the progressive lesions.

### The Vulnerable Lesions

Thin-cap fibroatheromas and ruptures are hallmarked by a peak in T-cell infiltration in the adventitia underneath the culprit lesion (Figures 3 through 9). The thin cap remains devoid of T cells, and the number of T-helper cells decreases, resulting in an approximate 1:1 CD4/CD8 cell ratio. Non-Th1 cells remain the dominant T-helper lineage in

the vulnerable phase, due to doubling of the number of non-Th1 cells (Figure 6). Dispersed memory T cells and naïve T cells are abundantly present in the media and adventitia near the vasa vasorum. Absence of CD45RO/CCR7 double-positive cells indicates that all CD45RO<sup>+</sup> T cells within the lesion and infiltrates are effector memory T cell and the only few central memory T cells are identified in the aortic wall located within the vasa vasorum of the adventitia (Figure 10).

A unique finding in the vulnerable lesions is the appearance of B cells and occasional plasma cells in tertiary folliclelike structures. Staining for CXCL13, a homeostatic, lymphorganogenic chemokine that is critical for organization of folliclelike structures, shows CXCL13 expression exclusively in vulnerable lesions (viz, no CXCL13 staining was found in the other stages of the disease) and reveals a particular staining pattern of a dendritic network with extension from the follicles (Figure 9). Additional staining

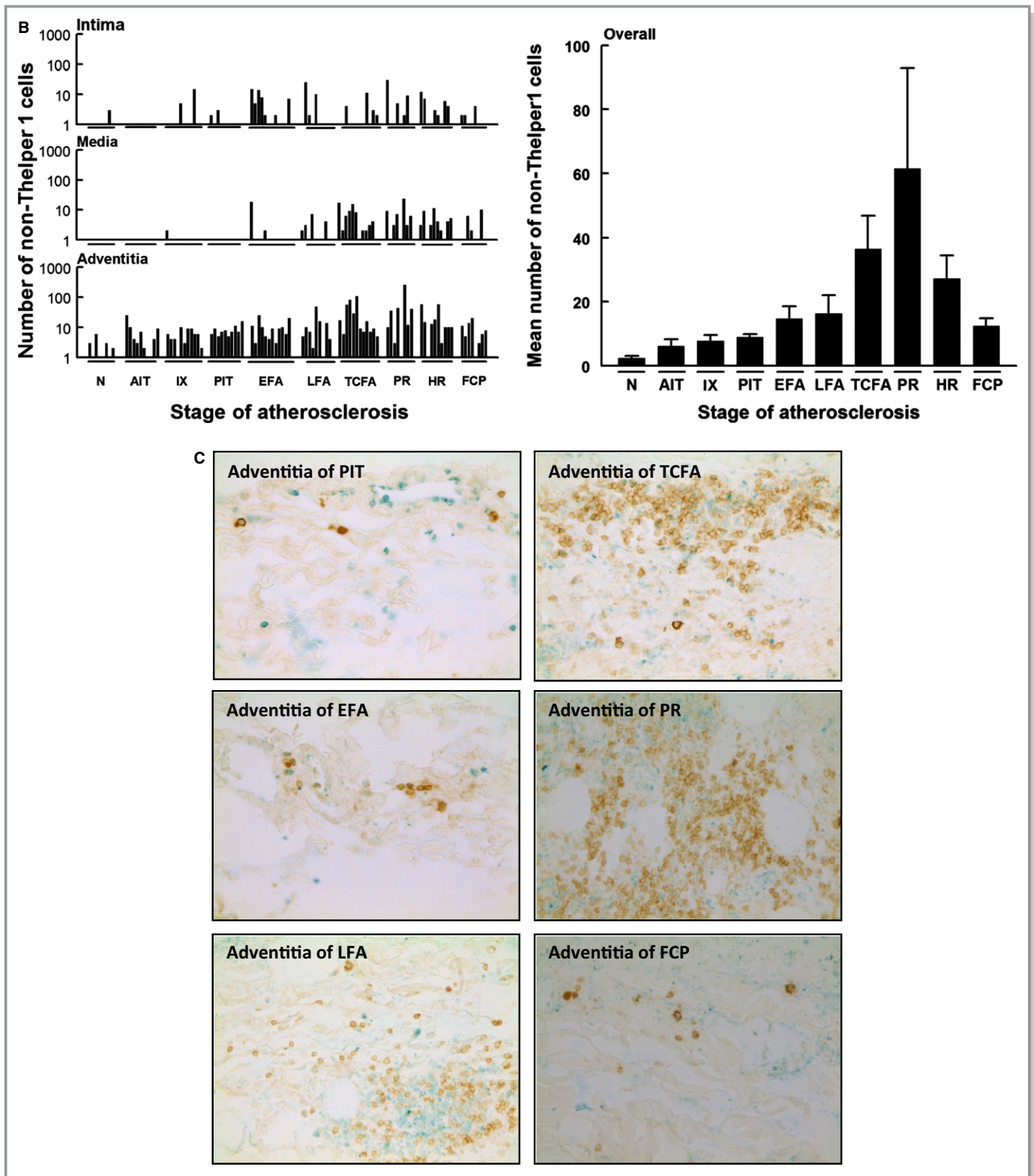


**Figure 6.** *Continued*

for mature B cells (CD2) and activation-induced cytidine deaminase was mainly negative, indicating the lack of B-cell maturation. Scattered FoxP3<sup>+</sup> T cells are found within the

intima and underlying adventitia in 2 of 9 aortic sections of thin-cap fibroatheroma (Figure 4). On the other hand, Th17 cells are absent in vulnerable lesions.

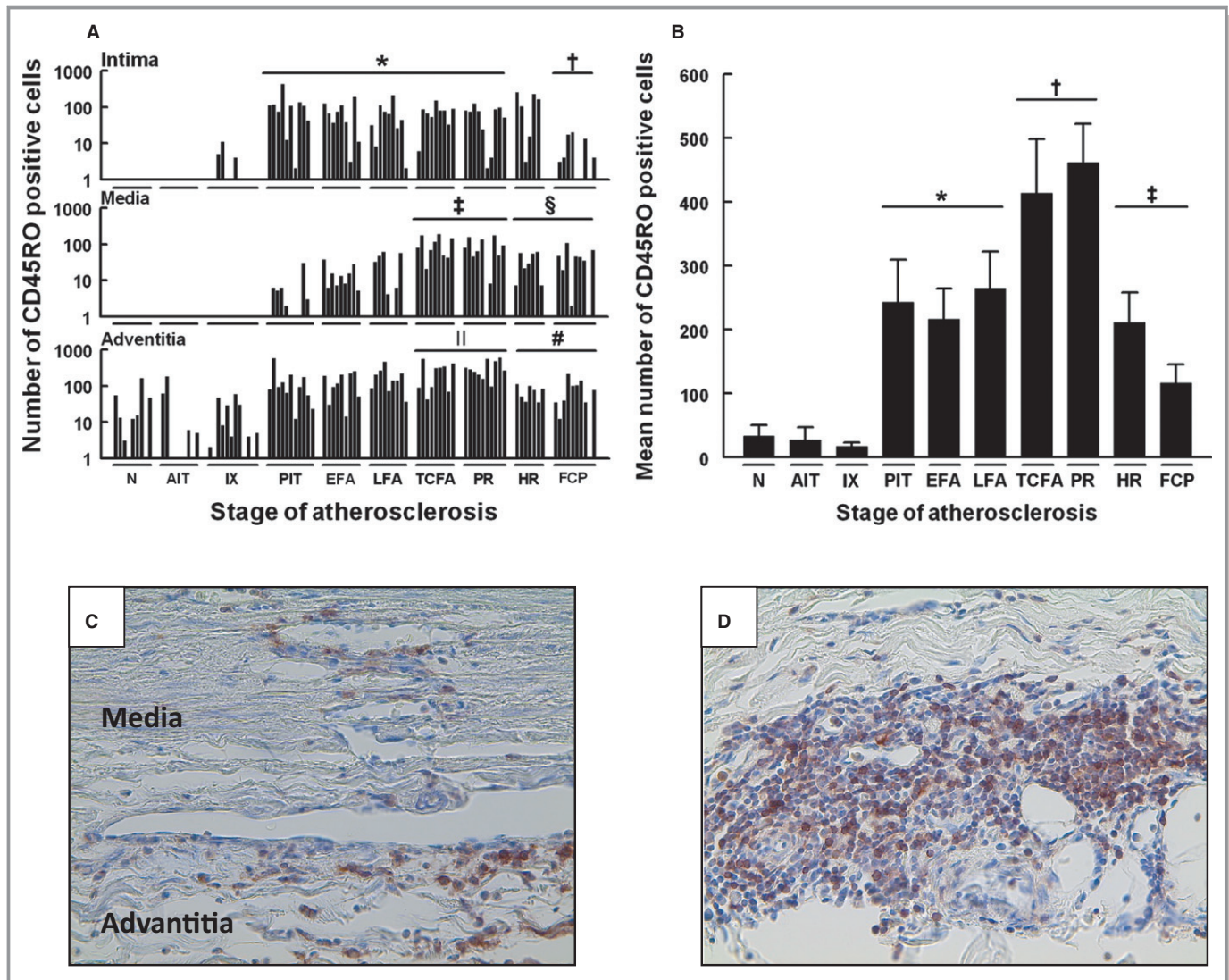


**Figure 7.** Number of memory T cells within the various layers of the aortic wall. A, Progressive atherosclerotic lesions and vulnerable plaques represent a high amount of CD45RO<sup>+</sup> T cells in the intima (\**P*<0.011). Only fibrotic calcified lesions show a significant decrease compared to vulnerable lesions (<sup>†</sup>*P*<0.001). In comparison with normal, AIT and IX (*viz.* Nonprogressive intimal lesions) the media and adventitia show an increasing number of memory T cells within progressive atherosclerotic lesions followed by a significant rise within the vulnerable plaques and a significant decrease as the lesions stabilize (<sup>†</sup>*P*<0.0001; <sup>‡</sup>*P*<0.0001; <sup>§</sup>*P*<0.0001; and <sup>||</sup>*P*<0.0001). B, Memory T cells significantly increase in number within progressive and vulnerable lesions followed by a decrease in stabilized lesions (\**P*<0.0001; <sup>†</sup>*P*<0.0001 and <sup>‡</sup>*P*<0.0001). C and D, Illustrative images of the CD45RO staining of, respectively, the adventitia of a LFA and the adventitia of a TCFA corresponding with the presented graphs. All sections were developed with DAB and counterstained with Mayer’s hematoxylin. The vertical axis of (A) is presented as a log-scale. The solid bars in (A) represent the number of CD45RO<sup>+</sup> T cells within the various layers of 1 aortic plaque. The solid bars in (B) represent the mean number of CD45RO<sup>+</sup> T cells within the entire aortic wall of 1 aortic plaque ±SEM. Total number of cases in (A) and (B): 95 (N [9], AIT [9], IX [12], PIT [11], EFA [9], LFA [9], TCFA [9], PR [10], HR [7] and FCP [10]). AIT indicates adaptive intimal thickening; EFA, early fibroatheroma; HR, healed rupture; FCP, fibrotic calcified plaque; IX, intimal xanthoma; LFA, late fibroatheroma; N, normal; PIT, pathological intimal thickening; PR, plaque rupture; TCFA, thin-cap fibroatheroma. For a detailed description concerning the classification, see the Materials and Methods section. All images were taken at ×400 magnification.

### Stabilized Lesions

Healing plaque ruptures exhibit a dramatic decrease in T cells (*P*<0.001), naïve T cells, and disappearance of B cells and plasma cells (Figures 2 through 9). The decline in T cells is greater for the CD4<sup>+</sup> cells than for the CD8<sup>+</sup> cells

for all vascular layers. Within the thin-cap fibroatheroma, non-Th1 cells dominate over Th1 with a 5-fold-increase, and in stable lesions the Th1/non-Th1 cell ratio returns to 1:2 as seen in normal aortas (Figure 3B). The decline in memory T cells predominantly reflects a reduction localized to the intima (*P*<0.01). The overall number of memory T cells in

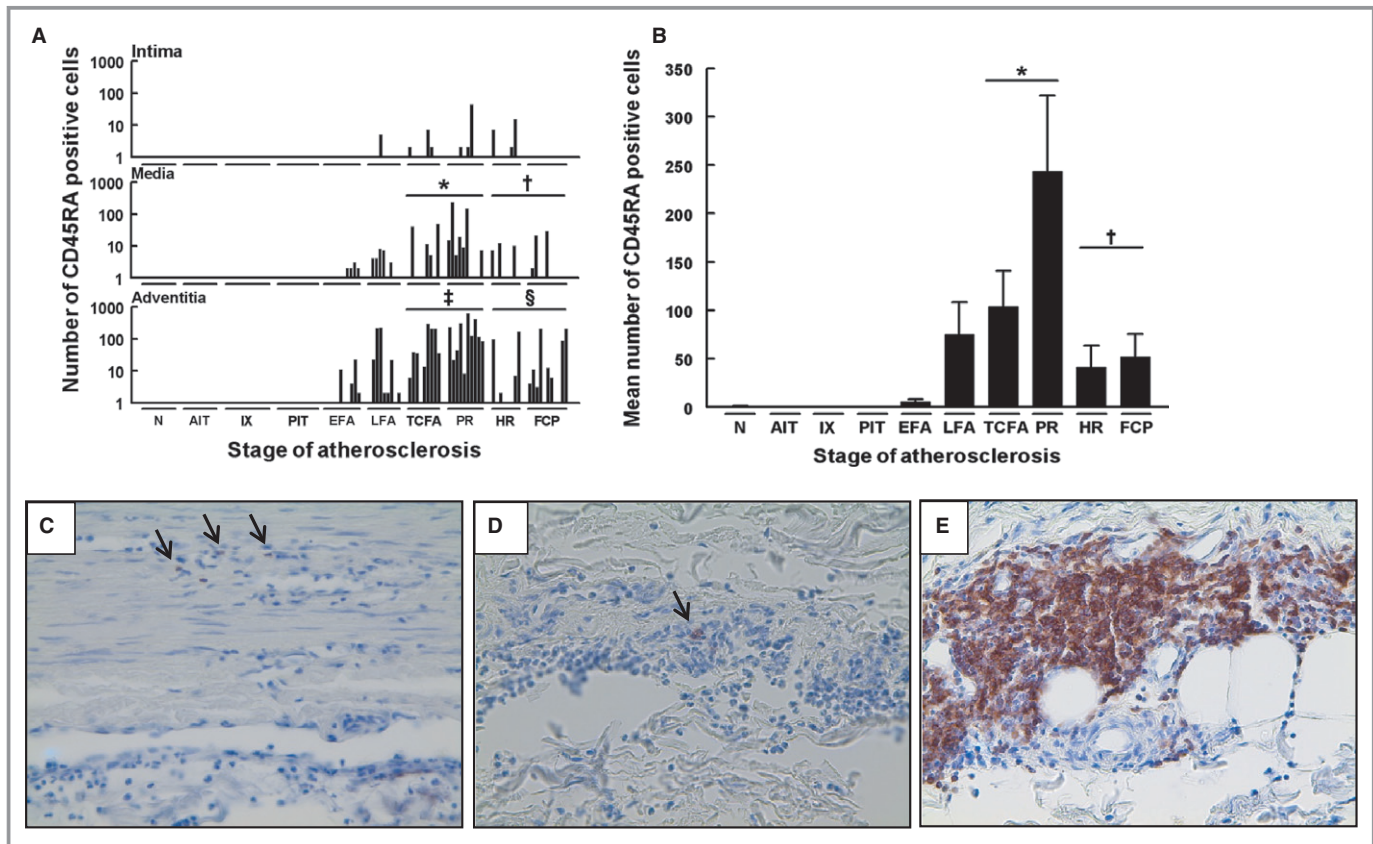


**Figure 8.** Number of naïve T cells within the various layers of the aortic wall. A, Limited numbers of CD45RA<sup>+</sup> T cells are detected in the intima of vulnerable lesions. However, the media and adventitia contain a significant increase in naïve T cells within the vulnerable lesions compared to the progressive lesions (EFA and LFA) followed by a decrease in stabilized lesions (\* $P < 0.001$ ; † $P < 0.006$ ; ‡ $P < 0.0001$ ; and § $P < 0.0001$ ). B, Naïve T cells increase significantly in number in vulnerable plaques (\* $P < 0.0001$ ) and decrease dramatically in number when the lesions stabilize († $P < 0.0001$ ). The vertical axis of (A) is presented as a log-scale. The solid bars in (B) represent the mean number of CD45RA<sup>+</sup> T cells within the entire aortic wall of 1 aortic plaque  $\pm$  SEM. Total number of cases in (A) and (B): 97 (N [9], AIT [9], IX [11], PIT [11], EFA [10], LFA [9], TCFA [9], PR [10], HR [8], and FCP [11]). AIT indicates adaptive intimal thickening; EFA, early fibroatheroma; HR, healed rupture; FCP, fibrotic calcified plaque; IX, intimal xanthoma; LFA, late fibroatheroma; N, normal; PIT, pathological intimal thickening; PR, plaque rupture; TCFA, thin-cap fibroatheroma. For a detailed description concerning the classification, see the Materials and Methods section. All images were taken at  $\times 400$  magnification.

the media and adventitia remains stable. Native T-cell numbers are highly variable. The folliclelike structures vanish and CXCL13 disappeared from the arterial wall. No regulatory T cells or Th17 cells are detected in the stabilized lesions.

## Discussion

A wealth of preclinical evidence supports a critical role of the adaptive immunity in the initiation and progression of atherosclerosis.<sup>17,18</sup> This study, based on histological observations in human aorta sections, confirms extensive and progressive involvement of cellular components of the

adaptive immune response in atherosclerosis.<sup>19</sup> Findings point to profound changes in the nature of the response in the lead-up to plaque destabilization and show extinguishing of inflammatory processes upon plaque stabilization. This study reveals fundamental differences between the human atherosclerotic disease and mouse models of the disease, particularly with respect to a very limited presence of regulatory T cells, absence of Th17 cells throughout the atherosclerotic process, and lack of B cells in the early-, intermediate-, and final stages of the process.

Insight into the atherosclerotic process greatly depends on observations from murine models of the disease.<sup>20</sup> Indeed, genetically modified mouse models have been critical for

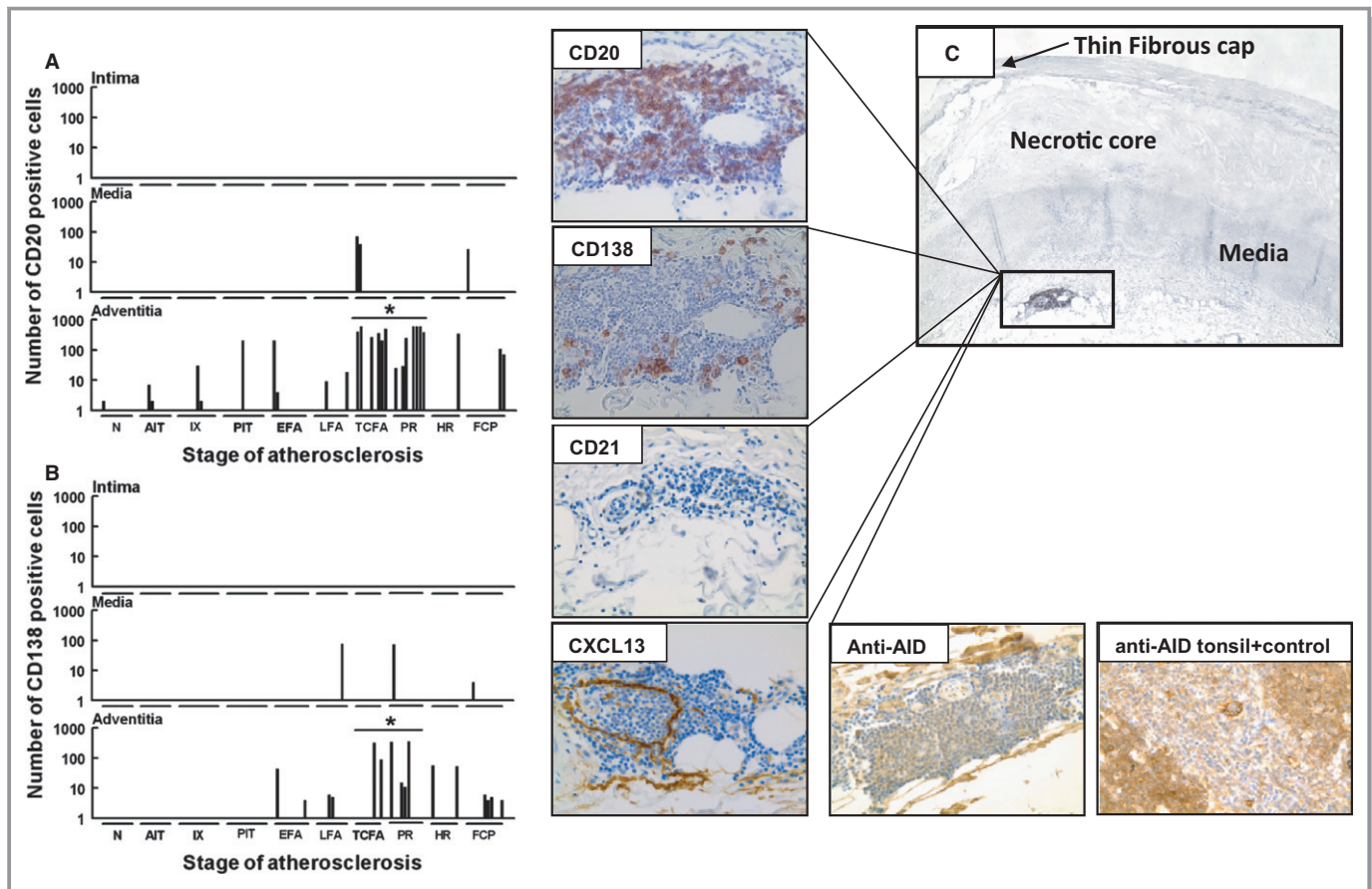


**Figure 9.** Number of CD20<sup>+</sup> B cells and CD138<sup>+</sup> plasma cells in the various layers of the aortic wall. The intima and media of the aortic wall remain largely deprived of CD20<sup>+</sup> B cells and CD138<sup>+</sup> plasma cells (A and B, respectively), although incidental B cells are found in the adventitia. There is a significant increase in the amount of B cells and plasma cells in the adventitia in close proximity to the intimal plaque in the vulnerable lesions compared to the prior phase (\**P*<0.0001 and \**P*<0.003). Total number of cases: 97 (N [9], AIT [9], IX [11], PIT [11], EFA [10], LFA [9], TCFA [9], PR [10], HR [8], and FCP [11]). C, An adventitial follicle in a thin-cap fibroatheroma consecutively stained for CD20, CD21, and CXCL13. Notice the abundance of (CD21-negative) B cells clustered around the CXCL13 positive radiating pattern of tubelike structures. Anti-activation-induced cytidine deaminase (AID) stained negative within the adventitial infiltrates. Due to the disturbing amount of background staining, a high-resolution image of a positive control for the anti-AID staining in a human tonsil is provided to illustrate the mature B cell. All images were taken at ×400 magnification. All sections were developed with Diaminobenzidine (DAB) and counterstained with Mayer's hematoxylin. The vertical axis is presented as a log-scale. The solid bars represent the number of CD20<sup>+</sup> B cells or CD138<sup>+</sup> plasma cells within the various layers of 1 aortic plaque. AIT indicates adaptive intimal thickening; EFA, early fibroatheroma; HR, healed rupture; FCP, fibrotic calcified plaque; IX, intimal xanthoma; LFA, late fibroatheroma; N, normal; PIT, pathological intimal thickening; PR, plaque rupture; TCFA, thin-cap fibroatheroma. For a detailed description concerning the classification, see the Materials and Methods section.

understanding the atherosclerotic process. Yet, by virtue of the metabolic adaptations in the lipoprotein metabolism, necessary to induce atherosclerotic lesion formation, the process in these animals is essentially lipid driven (a situation that may not fully mimic the human situation).<sup>21,22</sup> Translation of rodent findings is further obscured by critical dependence on genetic backgrounds with Th1-dominated immune responses in order for atherosclerosis to develop; by the fundamental and intrinsic differences in inflammatory and immune responses between mice and humans; and by failure of the experimental lesions to progress to culprit lesions (vulnerable plaque) formation.<sup>7,23,24</sup> Consequently, informa-

tion provided by these models may be biased, and is incomplete at least with respect to vulnerable lesions. As a result, the preclinical observations may not directly translate to the human situation.<sup>8,9</sup>

Data on human atherosclerosis are also limited, a situation largely reflecting the fact that most observations are made on material obtained during surgical procedures (eg, endarterectomy). This material typically represents the final stage(s) of the disease and, in the case of an endarterectomy material, will not provide information on the outer media and the adventitia, both major interphases in vessel wall inflammation. With this in mind, we set up a biobank of aortic wall

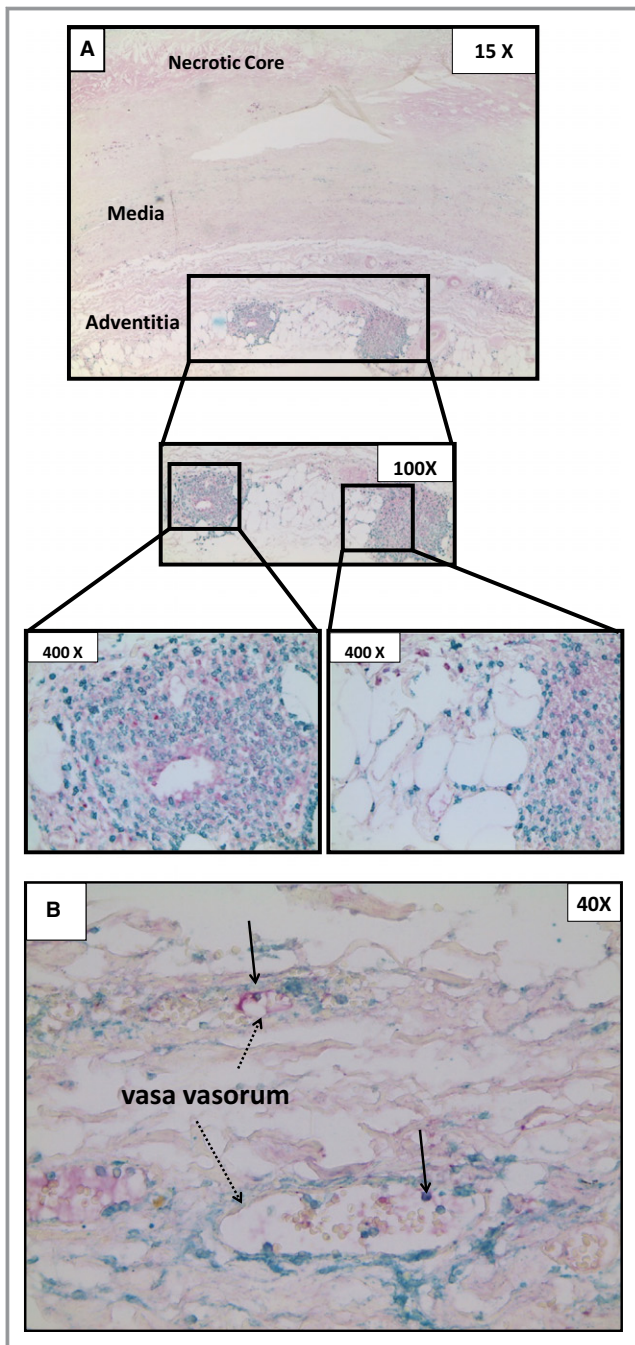


**Figure 10.** Thin-cap fibroatheroma stained for CD45R0/CCR7.<sup>16</sup> Immunohistochemical double staining for CCR7/CD45R0 was done to differentiate between effector memory T cells (CCR7<sup>-</sup>) and central memory T cells (CCR7<sup>+</sup>). A, The adventitia of the aortic wall containing a thin-cap fibroatheroma consists of numerous T cells in follicle-like structures. All the CD45R0<sup>+</sup> T cells (chromogen Ferangi blue) within the lesion and infiltrates are effector memory T cell (CCR7<sup>-</sup>; otherwise warp red [klinipath, Duiven, Netherlands]). Only a few cells stain positive for CCR7 but negative for CD45R0. B, The only few central memory T cells (CD45R0<sup>+</sup>/CCR7<sup>+</sup>) identified in the aortic wall are located within the vasa vasorum of the adventitia. The image was taken at  $\times 400$  magnification.

samples from organ grafts designated for transplantation. Material from this bank almost covers the full life span (5 to 80 years) and shows a nearly equal sex distribution. The relatively healthy premortal status of the donors is reflected by minimal use of statins and antihypertensive drugs. Classification was done for all individual tissue sections in the bank (viz, each individual tissue block was Movat and hematoxylin stained, and histologically staged using an established adapted version of the AHA classification system).<sup>12,13</sup> Modifications in the adapted classification system highlight specific critical morphological events in the final stages of the disease process. This allows for a more precise interpretation of processes occurring during plaque destabilization and subsequent healing. An earlier systematic evaluation of material in the biobank showed that the bank covers the full spectrum of atherosclerotic disease.<sup>12</sup> Exact morphologic descriptions and examples of the different lesions have been published and discussed previously.<sup>12</sup>

Immunohistochemical staining for CD3, CD4, and CD8 shows progressive T-cell accumulation during the atherosclerotic process. The earlier phases are dominated by diffuse cytotoxic T-cell infiltration, but progressive quantities of T-helper cells are found during progression of the disease, resulting in an increase in the CD4<sup>+</sup>/CD8<sup>+</sup> T-cell ratio during disease progression. These observations are in line with an earlier report on renal artery atherosclerosis, and with observations from other progressive inflammatory disorders.<sup>25,26</sup> Due to inherent limitations of paraffin-embedded tissue, we were unable to test whether these shifts reflect an (auto)immune phenomenon, as has been proposed in the context of advanced atherosclerotic disease.<sup>27,28</sup>

CD4/T-Bet double staining was used to identify Th1 cells. T-bet is the lineage-defining transcription factor for Th1 cells.<sup>29</sup> In the absence of Th17 and with minimal regulatory T cells throughout the atherosclerotic spectrum, we defined the CD4<sup>+</sup>/T-bet-negative cells as non-Th1 cells. Quantification of the Th1/non-Th1 ratio on the basis of the CD4/T-Bet double staining did not confirm Th1 dominance in the human atherosclerotic process. This may indicate that the presumed Th1 dominance in atherosclerosis reflects an artificial phenomenon related to the requirement of Th1-dominated backgrounds in mouse models in order for atherosclerosis to develop. Yet, alternative explanations are that identification based on T-Bet positivity underestimates the number of Th1 cells or, vice versa, that identification based on cytokine profiles overestimates the number of Th1 cells.<sup>30</sup>

Findings for the CD45R0 (T-memory cells) and CD45RA (naïve T cells) largely follow observations for other solid organs (predominance of T-memory cells) and extend those made in rodent models of atherosclerotic disease showing

increasing T-cell infiltration during disease progression, with a clear maximum during plaque destabilization followed by a rapid decline during plaque stabilization (plaque healing).<sup>31</sup> A remarkable and novel observation is the change in the inflammatory footprint that accompanies plaque destabilization, and that fully resolves during plaque stabilization. This change appears to precede plaque destabilization, and is confined to the area adjacent to the culprit lesion. On the cellular level, this change is characterized by a sharp increase in the number of T-helper cells, emergence of naïve T-cells, and the appearance of B cells and occasional plasma cells in tertiary folliclelike structures. B cells in the follicles are largely activation-induced cytidine deaminase and CD21 negative, indicating gross absence of B-cell maturation.<sup>32,33</sup> These observations suggest that signals promoting B-cell homing and follicle assembly accompany (and may even precede) plaque destabilization, but that essential signals critical for maturation of B cells are missing.

The chemokine CXCL13 is a pivotal homeostatic signal for follicle formation.<sup>34,35</sup> As for the appearance of folliclelike structures, we performed immunostaining for CXCL-13 and observed CXCL-13 expression exclusively in association with the folliclelike structures in the vulnerable lesions (viz, CXCL-13 was not detected in the other stages of the disease). CXCL13 distribution shows a remarkable radiating pattern of tubelike structures that may reflect expression in dendritic cells.<sup>36</sup>

In light of the remarkable association between CXCL13 and plaque instability, we tested an association between plasma CXCL13 levels and acute cardiovascular events (acute myocardial infarction) in plasma samples of the Mission study.<sup>36</sup> CXCL13 was largely undetectable, and no association was found between CXCL-13 and cardiovascular events (results not shown). Absence of such an observation may reflect the highly localized character of CXCL13 expression in the vulnerable lesion.

B cells are considered critical players in the atherosclerotic process, albeit their role (protective, detrimental) is still under debate.<sup>37,38</sup> Our findings of a very restricted presence of B cells in human atherosclerosis follow observations from Frostegård et al<sup>39</sup> Hence, these findings and gross absence of signs of B-cell maturation in the infiltrating B cells exclude an autocrine or paracrine role of B cells in the human atherosclerotic process. Yet, humoral factors released by B cells in paravascular lymph nodes or more distant locations may well be involved in the disease process.

Regulatory T cells were incidentally found in a subset of the vulnerable lesions, whereas Th17 cells were fully absent in the aortic sections. This latter observation follows results of a comprehensive analysis of cytokines in atherosclerotic wall samples that failed to detect interleukin-17 in all samples tested (detection threshold of the assay <1 pg/L).<sup>40</sup> Although these observations do not exclude a distant role for these cell

populations, they seem to contradict observations from murine models implying these cells as local key-players in the atherosclerotic process.

## Limitations

This study was performed on aortic sections of deceased individuals, as such the continuous data in this study are composed of incidental findings from a large series of patients and therefore may not necessarily reflect longitudinal data. Another limitation of the study is the fact the all findings are based on IHC using paraffin-embedded tissue sections. Although IHC has the advantage of showing the spatial relationships, multiple stainings are elaborative, and only allow for very limited marker sets. Consequently, findings in this study should be considered at a global level. That is, the apparent mismatch between the total number of CD3 counts and the sum of CD4 and CD8 may reflect abundance of other CD3-expressing populations such as NK and NK-T cells but also reflect technical limitations of IHC with different epitope availabilities and antibody efficacies. Yet, it is likely that the latter phenomena would equally apply to all tissue sections, and it is thus unlikely that this would influence the conclusions of the study.

In conclusion, this study shows clear changes in the cellular components of the adaptive immune system in anticipation of and during plaque destabilization. Observations suggest that changes in the inflammatory footprint precede and accompany plaque instability. It is tempting to speculate that delineation of this chain of events may provide clues for early culprit lesion detection and plaque stabilization.

## Disclosures

None.

## References

- Hansson GK. Inflammation, atherosclerosis, and coronary artery disease. *N Engl J Med*. 2005;352:1685–1695.
- Hansson GK, Libby P. The immune response in atherosclerosis: a double-edged sword. *Nat Rev Immunol*. 2006;6:508–519.
- Mallat Z, Taleb S, Ait-Oufella H, Tedgui A. The role of adaptive T cell immunity in atherosclerosis. *J Lipid Res*. 2009;50:S364–S369.
- Libby P, Ridker PM, Hansson GK. Inflammation in atherosclerosis: from pathophysiology to practice. *J Am Coll Cardiol*. 2009;54:2129–2138.
- Seok J, Warren HS, Cuenca AG, Mindrinos MN, Baker HV, Xu W, Richards DR, McDonald-Smith GP, Gao H, Hennessy L, Finnerty CC, López CM, Honari S, Moore EE, Minei JP, Cuschieri J, Bankey PE, Johnson JL, Sperry J, Nathens AB, Billiar TR, West MA, Jeschke MG, Klein MB, Gamelli RL, Gibran NS, Brownstein BH, Miller-Graziano C, Calvano SE, Mason PH, Cobb JP, Rahme LG, Lowry SF, Maier RV, Moldawer LL, Herndon DN, Davis RW, Xiao W, Tompkins RG. Genomic responses in mouse models poorly mimic human inflammatory diseases. *Proc Natl Acad Sci*. 2013;110:3507–3512.
- Weber C, Zernecke A, Libby P. The multifaceted contributions of leukocyte subsets to atherosclerosis: lessons from mouse models. *Nat Rev Immunol*. 2008;8:802–815.
- Mestas J, Hughes CCW. Of mice and not men: differences between mouse and human immunology. *J Immunol*. 2004;172:2731–2738.

8. Schulte S, Sukhova GK, Libby P. Genetically programmed biases in Th1 and Th2 immune responses modulate atherogenesis. *Am J Pathol.* 2008;172:1500–1508.
9. Dansky HM, Charlton SA, Sikes JL, Heath SC, Simantov R, Levin LF, Shu P, Moore KJ, Breslow JL, Smith JD. Genetic background determines the extent of atherosclerosis in ApoE-deficient mice. *Arterioscler Thromb Vasc Biol.* 1999;19:1960–1968.
10. De Boer OJ, Van Der Meer JJ, Teeling P, Van Der Loos CM, Van Der Wal AC. Low numbers of FOXP3 positive regulatory T cells are present in all developmental stages of human atherosclerotic lesions. *PLoS One.* 2007;2:e779.
11. Tavora F, Kutys R, Li L, Ripple M, Fowler D, Burke A. Adventitial lymphocytic inflammation in human coronary arteries with intimal atherosclerosis. *Cardiovas Pathol.* 2009;19:61–68.
12. van Dijk RA, Virmani R, von der Thüsen JH, Schaapherder AF, Lindeman JHN. The natural history of aortic atherosclerosis: a systematic histopathological evaluation of the peri-renal region. *Atherosclerosis.* 2010;210:100–106.
13. Virmani R, Kolodgie FD, Burke AP, Farb A, Schwartz SM. Lessons from sudden coronary death: a comprehensive morphological classification scheme for atherosclerotic lesions. *Arterioscler Thromb Vasc Biol.* 2000;20:1262–1275.
14. de Boer OJ, Li X, Teeling P, Mackaay C, Ploegmakers HJ, van der Loos CM, Daemen MJ, de Winter RJ, van der Wal AC. Neutrophils, neutrophil extracellular traps and interleukin-17 associate with the organisation of thrombi in acute myocardial infarction. *Thromb Haemost.* 2013;109:290–297.
15. Chen L, Bea F, Wangler S, Celik S, Wang Y, Böckler D, Dengler TJ. Inhibition of IL-17A attenuates atherosclerotic lesion development in apoE-deficient mice. *J Immunol.* 2009;183:8167–8175.
16. Mackay CR. Dual personality of memory T cells. *Nature.* 1999;401:659–660.
17. Swirski FK, Nahrendorf M. Leukocyte behavior in atherosclerosis, myocardial infarction, and heart failure. *Science.* 2013;339:161–166.
18. Wigren M, Nilsson J, Kolbus D. Lymphocytes in atherosclerosis. *Clin Chim Acta.* 2012;413:1562–1568.
19. Libby P, Ridker PM, Hansson GK. Progress and challenges in translating the biology of atherosclerosis. *Nature.* 2011;473:317–325.
20. Kleemann R, Zadelaar S, Kooistra T. Cytokines and atherosclerosis: a comprehensive review of studies in mice. *Cardiovasc Res.* 2008;79:360–376.
21. Emerging Risk Factors Collaboration; Di Angelantonio E, Sarwar N, Perry P, Kaptoge S, Ray KK, Thompson A, Wood AM, Lewington S, Sattar N, Packard CJ, Collins R, Thompson SG, Danesh J. Major lipids, apolipoproteins, and risk of vascular disease. *J Am Med Assoc.* 2009;302:1993–2000.
22. Lichtman AH. Adaptive immunity and atherosclerosis: mouse tales in the AJP. *Am J Pathol.* 2013;182:5–9.
23. Huber SA, Sakkinen P, David C, Newell MK, Tracy RP. T helper-cell phenotype regulates atherosclerosis in mice under conditions of mild hypercholesterolemia. *Circulation.* 2001;103:2610–2616.
24. Ni M, Chen WQ, Zhang Y. Animal models and potential mechanisms of plaque destabilisation and disruption. *Heart.* 2009;95:1393–1398.
25. Kotliar C, Juncos L, Inserra F, de Cavanagh EM, Chuluyan E, Aquino JB, Hita A, Navari C, Sánchez R. Local and systemic cellular immunity in early renal artery atherosclerosis. *Clin J Am Soc Nephrol.* 2012;7:224–230.
26. Aoshiba K, Koinuma M, Yokohori N, Nagai A: Respiratory Failure Research Group in Japan. Differences in the distribution of CD4+ and CD8+ T cells in emphysematous lungs. *Respiration.* 2004;71:184–190.
27. Artemiadis AK, Anagnostouli MC. Apoptosis of oligodendrocytes and post-translational modifications of myelin basic protein in multiple sclerosis: possible role for the early stages of multiple sclerosis. *Eur Neurol.* 2010;63:65–72.
28. Hussein MR, Hassan HI, Hofny ER, Elkholy M, Fatehy NA, Abd Elmoniem AE, Ezz El-Din AM, Afifi OA, Rashed HG. Alterations of mononuclear inflammatory cells, CD4/CD8+ T cells, interleukin 1beta, and tumour necrosis factor alpha in the bronchoalveolar lavage fluid, peripheral blood, and skin of patients with systemic sclerosis. *J Clin Pathol.* 2005;58:178–184.
29. Oestreich KJ, Weinmann AS. T-bet employs diverse regulatory mechanisms to repress transcription. *Trends Immunol.* 2012;33:78–83.
30. de Boer OJ, van der Wal AC, Verhagen CE, Becker AE. Cytokine secretion profiles of cloned T cells from human aortic atherosclerotic plaques. *J Pathol.* 1999;188:174–179.
31. Alberts-Grill N, Rezvan A, Son DJ, Qiu H, Kim CW, Kemp ML, Weyand CM, Jo H. Dynamic immune cell accumulation during flow-induced atherogenesis in mouse carotid artery: an expanded flow cytometry method. *Arterioscler Thromb Vasc Biol.* 2012;32:623–632.
32. Houtkamp MA, de Boer OJ, van der Loos CM, van der Wal AC, Becker AE. Adventitial infiltrates associated with advanced atherosclerotic plaques: structural organization suggests generation of local humoral immune responses. *J Pathol.* 2001;193:263–269.
33. Hu Y, Ericsson I, Doseth B, Liabakk NB, Krokan HE, Kavli B. Activation-induced cytidine deaminase (AID) is localized to subnuclear domains enriched in splicing factors. *Exp Cell Res.* 2014;322:178–192.
34. Smedbakken LM, Halvorsen B, Daissormont I, Ranheim T, Michelsen AE, Skjelland M, Sagen EL, Folkersen L, Krohg-Sørensen K, Russell D, Holm S, Ueland T, Fevang B, Hedin U, Yndestad A, Gullestad L, Hansson GK, Biessen EA, Aukrust P. Increased levels of the homeostatic chemokine CXCL13 in human atherosclerosis—potential role in plaque stabilization. *Atherosclerosis.* 2012;224:266–273.
35. Daissormont I, Lipp M, Biessen EAL. The CXCL13-CXCR5 axis contributes to atherosclerosis development in LDLr<sup>-/-</sup> mice by regulating lymphocyte migration to perivascular lymph organs. *Cardiovasc Res.* 2010;87: S43–S44.
36. Liem SS, van der Hoeven BL, Oemrawsingh PV, Bax JJ, van der Bom JG, Bosch J, Viergever EP, van Rees C, Padmos I, Sedney MI, van Exel HJ, Verwey HF, Atsma DE, van der Velde ET, Jukema JW, van der Wall EE, Schalij MJ. MISSION!: optimization of acute and chronic care for patients with acute myocardial infarction. *Am Heart J.* 2007;153:e1–e11.
37. Ait-Oufella H, Herbin O, Bouaziz JD, Binder CJ, Uyttenhove C, Laurans L, Taleb S, Van Vré E, Esposito B, Vilar J, Sirvent J, Van Snick J, Tedgui A, Tedder TF, Mallat Z. B cell depletion reduces the development of atherosclerosis in mice. *J Exp Med.* 2010;207:1579–1587.
38. Caligiuri G, Nicoletti A, Poirier B, Hansson GK. Protective immunity against atherosclerosis carried by B cells of hypercholesterolemic mice. *J Clin Invest.* 2002;109:745–753.
39. Frostegård J, Ulfgren A-K, Nyberg P, Hedin U, Swedenborg J, Andersson U, Hansson GK. Cytokine expression in advanced human atherosclerotic plaques: dominance of pro-inflammatory (Th1) and macrophage-stimulating cytokines. *Atherosclerosis.* 1999;145:33–43.
40. Lindeman JH, Abdul-Hussien H, Schaapherder AF, Van Bockel JH, Von der Thüsen JH, Roelen DL, Kleemann R. Enhanced expression and activation of pro-inflammatory transcription factors distinguish aneurysmal from atherosclerotic aorta: IL-6 and IL-8 dominated inflammatory responses prevail in the human aneurysm. *Clin Sci.* 2008;114:687–697.